

The Influence of the Variable Excitation Wavelength on the Spectral Characteristics of the Light Generated by the Luminescent Layer Consisting of YAG: Ce Phosphor and PDMS

Jan Jargus

Department of Telecommunications, Faculty of Electrical Engineering and Computer Science,
VSB - Technical University of Ostrava, Ostrava, Czech Republic
Email: jan.jargus@vsb.cz

Jan Nedoma^a, Marcel Fajkus^a, Jan Vitasek^a, Radek Martinek^b, Vladimír Vasinek^a

^aDepartment of Telecommunications, Faculty of Electrical Engineering and Computer Science,
VSB - Technical University of Ostrava, Ostrava, Czech Republic

^bDepartment of Cybernetics and Biomedical Engineering, Faculty of Electrical Engineering and Computer Science, VSB
- Technical University of Ostrava, Ostrava, Czech Republic

Email: {jan.nedoma, marcel.fajkus, jan.vitasek, radek.martinek, vladimir.vasinek}@vsb.cz

Abstract—In this work, we explored the changes in the spectral characteristics of the light generated by the luminescent layer containing YAG: Ce phosphor and polydimethylsiloxane (PDMS) in relation to a variable excitation wavelength of the light emitted from the monochromator. We created two types of test samples with a defined thickness of the luminescent layer and with a defined weight ratio of phosphor (cerium-doped yttrium aluminum garnet - YAG:Ce) in PDMS (Dowsil SE 1740). The correlated color temperature (CCT) of the first (second) type of samples ranged from 4387 to 6905 K (from 4923 to 8213 K) for excitation wavelengths of 425 - 445 nm (435 - 460 nm), respectively. The results revealed that this method can be used to design white light sources with an adjustable CCT.

Index Terms—CCT, PDMS, Spectral characteristic, YAG: Ce phosphor

I. INTRODUCTION

Phosphor as a light converter has been used in many lighting applications for a long time. Phosphor can be inserted into different host materials, thereby forming different types of luminescent layers. Phosphor-in-glass (PiG) based white light-emitting diodes (WLEDs) are presented in [1-4] and the advantages of composite phosphor ceramic are described in [5]. In our research, we used a luminescent layer composed of phosphor and PDMS.

PDMS is one of the outstanding representatives of the silicone materials, primarily because of its many excellent chemical and physical properties [6]. Some cases of the utilization phosphor doped PDMS are shown below.

The investigation of phosphor-doped polymer films for thermometry applications are studied in [7-9], and an optical probe for the detection of dissolved carbon dioxide based on a PDMS luminescent sensor membrane is shown in [10]. Authors team of article [11] describe the fabrication of a luminescent PDMS film with CaZnOS: Mn²⁺ phosphor. Other authors present a fabrication of GaN-based white light-emitting diodes with phosphor-doped PDMS substrate [12]. Another lighting applications with the mixture of phosphor and PDMS are mentioned in papers [13-14].

We used phosphor with cerium-doped yttrium aluminum oxide garnet particles (Y₃Al₅O₁₂: Ce or YAG: Ce; Phosphor Technology Ltd) in our experiments. The trade name of this phosphor is QMK58/F-U2, and we use the abbreviation U2 in this paper. The absorption of a narrow blue excitation light that is converted by the YAG phosphor to the range of approximately 500 to 700 nm is one of the possibilities of white light production. Since a portion of blue excitation light remains unchanged by the phosphor, the combination of this residue blue light with converted broadband light is perceived by the human eye as white light [15].

Numerous publications deal with the issue of YAG phosphors. Optical properties of macroporous Y₃Al₅O₁₂ crystals doped with rare earth ions (Ce, Eu, Sm, and Pr) are studied in [16]. Preparation of Y₃Al₅O₁₂:Ce powders by microwave-induced combustion process and their luminescent properties are discussed in [17] and the authors of paper [18] reviewed methods for synthesis and properties of phosphors based on aluminum yttrium garnets activated by rare-earth elements for white LEDs.

An important parameter of white light is the CCT and many researchers deal with the problem of the CCT tuning.

Manuscript received August 6, 2018; revised April 1, 2019.

For example, color temperature tunable white LED is described in [19]. Tuning by mixing of RGB colors is discussed in [20-22], and development of CCT tunable LED lighting system using red-blue-white LED is presented in [23]. White organic light-emitting diodes (WOLEDs) in a parallel tandem configuration with common injection electrodes allowed to tune CCT are shown in [24], and other tunable WOLEDs are presented in [25-26]. The different strategies for color tuning of upconversion emission were explored in [27-29].

In our research, we examined the effect of variable excitation wavelengths on the spectral characteristics of light generated by YAG:Ce phosphor in PDMS. We used a monochromator as a light source of variable wavelengths. The influence of variable excitation wavelengths on the properties of white light has already been investigated for lanthanide polymers [30-32]. This influence has not been studied for the luminescent layer consisting of YAG:Ce phosphor and PDMS. We found that the excitation wavelength strongly affects the CCT of the light generated by the luminescent layer, which means that this approach offers the opportunity to create alternative white light sources with a selected range of CCT values.

II. METHODS

The human eye has the color perception thanks to red, green and blue retina cones, which are sensitive to the corresponding colors. In 1931, Commission Internationale de l'Eclairage (CIE) determined color-matching functions $\bar{x}(\lambda)$, $\bar{y}(\lambda)$, and $\bar{z}(\lambda)$, which are related to the red-sensitive, green-sensitive, and blue-sensitive cones, respectively [33] (see Fig. 1).

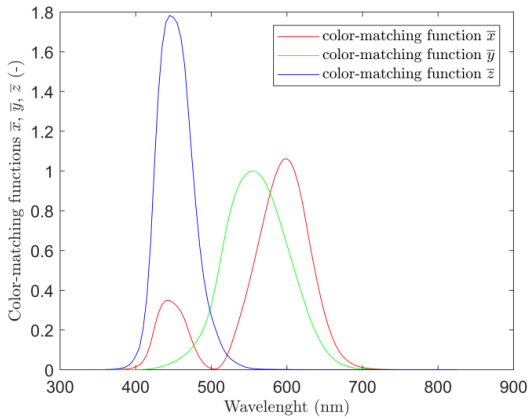


Figure 1. Color-matching functions, (CIE 1931) [39].

A light source with the $P(\lambda)$ emission spectrum produces the tristimulus values X , Y , Z , which characterize the color perception of this light source $P(\lambda)$ in the eye. The equations for calculating tristimulus values X , Y and Z are given below:

$$X = \int_{\lambda} \bar{x}(\lambda)P(\lambda) d\lambda \tag{1}$$

$$Y = \int_{\lambda} \bar{y}(\lambda)P(\lambda) d\lambda \tag{2}$$

$$Z = \int_{\lambda} \bar{z}(\lambda)P(\lambda) d\lambda \tag{3}$$

The chromaticity coordinates x and y determine the location in the chromaticity diagram. Pure colors are situated along the perimeter of the chromaticity diagram, in the center of which there is a white light area (see Fig. 2).

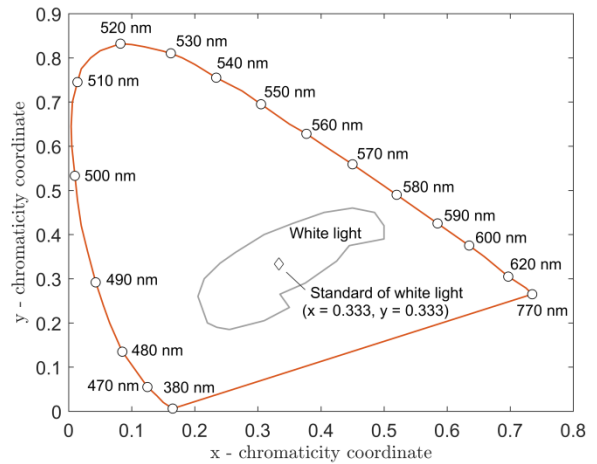


Figure 2. Scheme of the chromaticity diagram (x, y), (CIE, 1931).

The equations for calculation of the chromaticity coordinates from the tristimulus values are:

$$x = \frac{X}{X + Y + Z} \tag{4}$$

$$y = \frac{Y}{X + Y + Z} \tag{5}$$

$$z = \frac{Z}{X + Y + Z} = 1 - x - y \tag{6}$$

The Planckian black-body radiation spectrum is used as a standard for white light. The radiation of the black-body is situated in the (x, y) chromaticity diagram, and its location is called Planckian locus. With the increasing temperature of the Planck's black-body radiator (BBR), the Planckian locus moves from the red wavelength range towards the white central part of the chromaticity diagram, as shown in Figure 3. We can see that the BBR has temperatures in the range between 2400 and 10000 K for the white region of the chromaticity diagram [34].

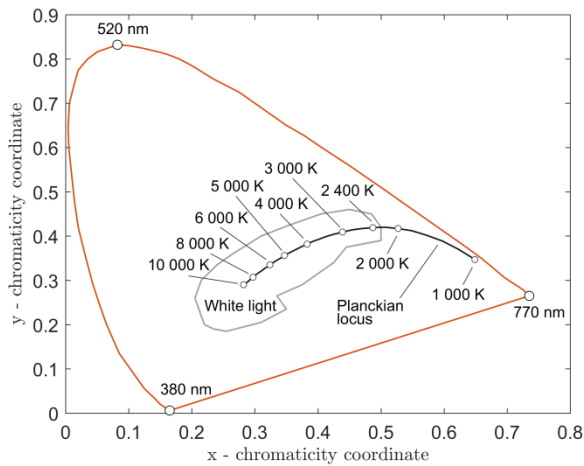


Figure 3. Scheme of Planck's black-body radiator [39].

The temperature of the BBR is closely related to the color temperature (CT), which is defined by using the Planckian locus. A white light source with the same chromaticity location as the BBR has the CT equal to the temperature of this BBR. The CCT is used in cases when the color of a white light source is different from the Planckian locus. The CCT value of a white light source is equal to the temperature of a BBR whose color is closest to the color of the white light source [34].

III. EXPERIMENTAL PART

A. Preparing of the Samples

We prepared 20 samples of the mixture of phosphor U2 and PDMS (Dowsil SE 1740, Dow Corning; we used the abbreviation SE 1740 in this paper). First ten samples had a weight ratio of 2:3 (U2:SE 1740) and the next ten samples had a weight ratio of 1:2 (U2:SE 1740). These samples were prepared for the experiment in several steps. First, we poured the components A SE1740 and B SE1740 in a weight ratio 1:1 into a beaker, and we mixed the mixture for 30 s by hand. Then we cooled it down to 5 °C to remove bubbles. After 120 minutes, we removed the beaker with this mix from the fridge, and we weighed twice 3.000 ± 0.002 g of this mixture into two test tubes. Then, we added 2.000 ± 0.002 g (1.500 ± 0.002 g) of the phosphor U2 to the test tube 1 (test tube 2), respectively. After that, both test tubes were placed in a laboratory shaker, where they were rotated and shaken for 300 minutes to ensure homogenization of the mixture. For the production of the first ten samples (second ten samples), 0.200 ± 0.002 g of the mixture of SE1740 and U2 from the test tube 1 (test tube 2) were applied to individual microscope slides. Then, each microscope slide was rotated for 60 seconds at 480 rpm (revolutions per minute), causing a thin film of the mixture to form in the middle of the microscope slide. We placed these samples in an electric furnace where they were cured at 90 °C for 30 minutes.

B. Setup of the Monochromator

In our research, we used the light emitted from the exit slit of the monochromator with the set wavelength in the

range of 425 – 475 nm and with FWHM = 25 nm. The light source for the monochromator was a 150 W halogen lamp LSH102 with a power supply LSN111. The spectrum of the 150 W halogen lamp is shown in Fig. 4.

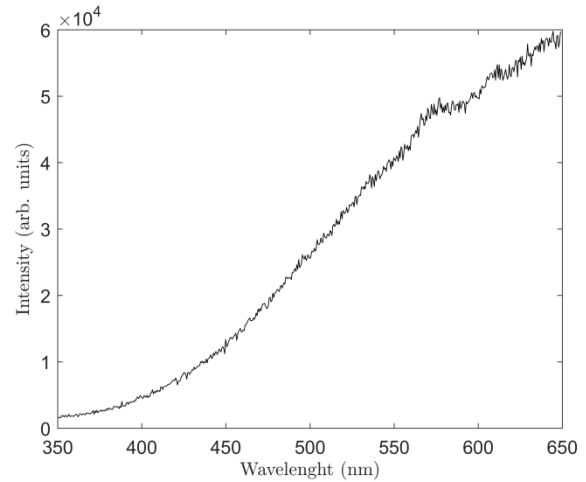


Figure 4. Spectrum of the halogen lamp in the range of 350 - 650 nm.

The spectral dependence of the light intensity of the halogen lamp (see Fig. 4) influences the spectral dependence of the output light. This situation might affect the measurement results. Therefore, for our next measurement, we needed a constant output optical power. We chose the light intensity of $6.92 \mu\text{W}$ emitted from the monochromator for a set wavelength of 425 nm as a reference. With gradual extension of the set wavelength of the light (using a 1 nm step), we gradually reduced the supply voltage of the halogen lamp to ensure that the output power of the emitted light remains the same (or only slightly variable). This setting of the halogen lamp supply voltage was recorded, and then used for all our measurements to provide a stable output power $6.92 \pm 0.01 \mu\text{W}$.

C. Experimental Setup

The measuring equipment consisted of the intense 150 W Lamp Housing LSH102, Halogen Lamp Power Supply LSN111, Omni- λ 150 Grating Monochromator, sample holder, optical fiber M28L01-IC 400 μm 0,39NA, spectrophotometer AvaSpec-HS2048, and a PC with required software (see Fig. 5).

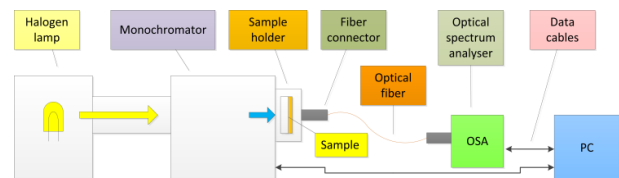


Figure 5. Scheme of the experimental setup.

D. Spectral Measurements

Spectral measurements were repeatedly performed. Samples were sequentially inserted into a specially prepared holder, and the individual measurements were done. We investigated the spectral properties of our samples for excitation wavelengths in the range of 425 - 475 nm (a part of purple and blue light) with 1 nm

measurement step. We recorded successive changes of the CCT and chromaticity coordinates, and we also recorded spectra of samples for selected wavelengths. See the graphs of the shifts of the CCT and chromaticity coordinates related to the change of the excitation wavelength in Fig. 6. For a better overview, the following Fig. 7 shows the curves corresponding to wavelengths 435 to 475 nm.

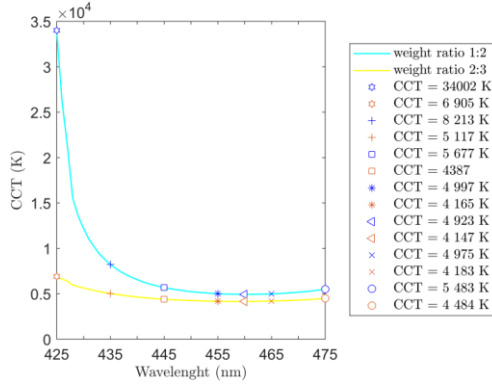


Figure 6. Curves of the dependencies of the average CCT values corresponding to the excitation wavelengths in the range of 425 - 475 nm.

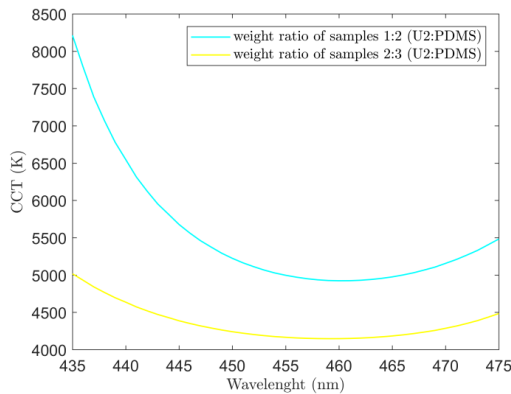


Figure 7. Curves of the dependencies of the average CCT values corresponding to the excitation wavelengths in the range of 435 - 475 nm.

The graph of the shifts of the chromaticity coordinates is presented in Fig. 8.

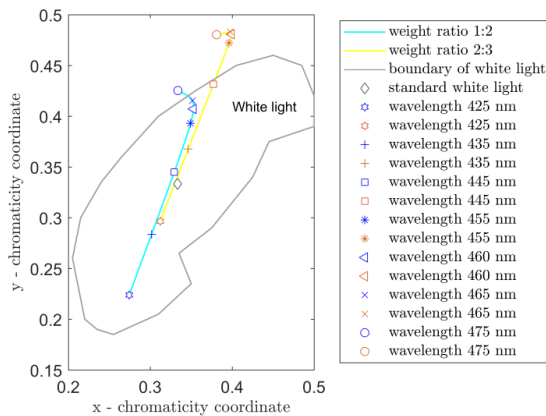


Figure 8. Shifts of the chromaticity coordinates for the range of excitation wavelengths 425 - 475 nm.

Significant values of Fig. 6 and Fig. 8 are shown in Table I.

TABLE I. THE VALUES OF THE CCT AND THE CHROMATICITY COORDINATES FOR THE SELECTED EXCITATION WAVELENGTHS.

wavelength (nm)	Weight ratio (U2:PDMS)					
	CCT (K)	chromat. coordinates		CCT (K)	chromat. coordinates	
		x (-)	y (-)		x (-)	y (-)
425	34002	0.274	0.224	6905	0.312	0.297
435	8213	0.302	0.284	5117	0.346	0.368
445	5677	0.329	0.345	4387	0.377	0.432
455	4997	0.349	0.393	4165	0.396	0.472
460	4923	0.353	0.407	4147	0.399	0.481
465	4975	0.352	0.415	4183	0.398	0.483
475	5483	0.334	0.425	4484	0.381	0.480

The curves of the samples of both concentrations are approaching the standard white light for some excitation wavelengths (see Fig. 8). Samples with a weight ratio of 1:2 (2:3) are the closest to this standard illuminant for the excitation wavelength of 443 nm (430 nm), respectively. Throughout our research, we measured the spectrum of all samples, but for a better overview, we used the average values of the samples with the same weight ratio phosphor in PDMS. The spectra of these average values are in Figures 9 - 11. For better clarity and comparison, we chose the spectra for excitation wavelengths that are associated with extreme points on the curve showing the dependence of the CCT on wavelengths, thus for the wavelengths of 425 nm (Fig. 9), 460 nm (Fig. 10), and 475 nm (Fig. 11).

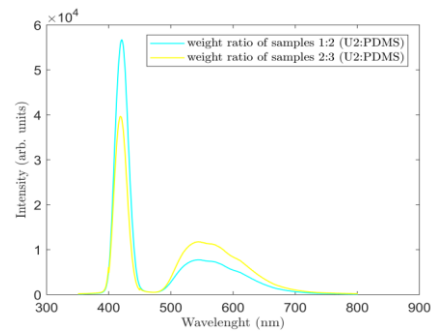


Figure 9. Comparison of the spectrum of samples with a weight ratio 1:2 and 2:3 (U2:PDMS) for the excitation wavelength of 425 nm.

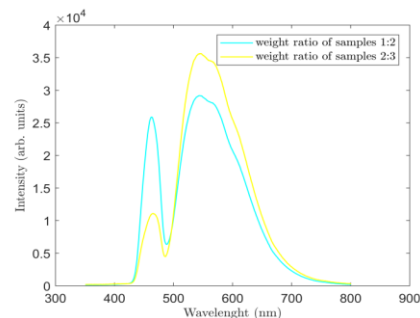


Figure 10. Comparison of the spectrum of samples with a weight ratio 1:2 and 2:3 (U2:PDMS) for the excitation wavelength of 460 nm.

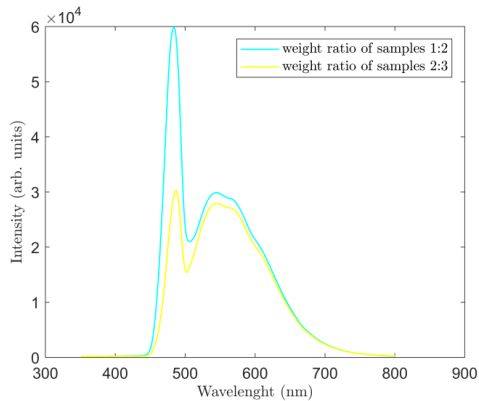


Figure 11. Comparison of the spectrum of samples with a weight ratio 2:3 and 1:2 (U2:PDMS) for the excitation wavelength of 475 nm.

After spectral measurements, we used the LPT 3113i-T microscope to measure the thickness of the samples' layers (see Fig. 12).

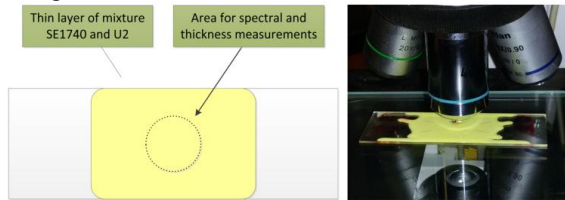


Figure 12. Scheme of the sample (left) and a photo of the microscopic measurement of the layer thickness (right).

The thickness of the layer was determined by a difference of the measured values identifying the upper and lower planes of the layer. The average values of the measured layer thickness were $126 \pm 2 \mu\text{m}$ ($119 \pm 2 \mu\text{m}$) for samples with the weight ratio U2 and PDMS 2:3 (1:2), respectively.

IV. DISCUSSION

The conversion of "narrow blue" light using the phosphor into broadband light depends strongly on the excitation wavelength (see Fig. 9 - 11). Each phosphor has a certain optimum excitation wavelength, in which the light is converted with the highest efficiency. With the increasing percentage of excitation light corresponding to the wavelength for which the phosphor has the highest efficiency, the conversion efficiency of the broadband light proportionally increases, resulting in a simultaneous reduction of the CCT. In our case, from the dependence CCT curve to the excitation wavelength of light, we can assume that phosphor U2 has the highest conversion efficiency for the excitation wavelength of about 460 nm (see Fig. 7).

This dependence of the conversion efficiency of the phosphor on the excitation wavelength of the light can be utilized in a "reasonable range" for tuning the desired CCT (see Fig. 6 and Fig. 8).

The CCT value of the light emitted from the sample also depends on the concentration of phosphor contained in the layer (see Fig. 7 - 8). We can deduce from the graphs that the CCT decreases with the increasing concentration of the phosphor in the luminescent layer of the sample.

For a comparison, the spectrum of the samples with different weight ratios 1:2 and 2:3 (U2:PDMS) is shown for the three excitation wavelengths 425 nm, 460 nm, and 475 nm in Fig. 9 - 11. The spectrum with the excitation wavelength of 425 nm indicates that only a small portion of violet light is transformed into broadband light. We can see that samples with a weight ratio 2:3 (yellow color), which contains a larger amount of phosphor than the samples with a weight ratio 1:2 (cyan color), converts a larger amount of excitation violet light into a broadband light with the range of wavelengths of about 500 - 700 nm (see Fig. 9). The spectrum with excitation wavelengths of 460 nm indicate that much of the blue light has been transformed into a wideband area of 500 - 700 nm, and this conversion is again more detectable in the samples (yellow color) with a higher total phosphor content (see Fig. 10). When looking at the last shown spectrum with the excitation wavelength of 475 nm, you can see that the samples of yellow color compared to the samples of cyan color convert a more significant portion of the excitation blue light into the broadband region (see Fig. 11). We also see that the light conversion is weaker for this wavelength than for the wavelength of 460 nm (see Fig. 10 - 11).

Fig. 9 shows the location of the light emitted from the sample depending on the excitation wavelength. When you look at the curve of the samples with weight ratio 2:3 (U2:PDMS), you can see that using an excitation wavelength in the entire range of 425 - 475 nm, we get beyond the white light boundary for longer wavelengths of this range. To remain in the white light range, for samples with a weight ratio of 2:3 we must use an excitation wavelength of approximately 425 - 445 nm (see Fig. 8). When looking at the curve of the samples with weight ratio of 1:2 (U2:PDMS), we see that in this case, we have increased the "tuning" range roughly twice as much as in the previous case, because for samples with a weight ratio of 1:2 we will remain inside the boundary of the white light even when used excitation wavelengths are in the range of about 425 - 465 nm.

Another result is that the shown graphs of the shifts of the chromaticity coordinates depending on their excitation wavelength are curves in the shape of lines, but they start to change their shape significantly in the vicinity of the excitation wavelength for which the phosphor achieves its maximum conversion efficiency (see Fig. 8). For the purpose of an adjustable CCT by means of excitation wavelength, it would therefore be desirable for this "tuning" to take place in the range of a certain minimum excitation wavelength (selected so that we are still in the white light region), with a high value of the CCT up to the maximum excitation wavelength at which the phosphor reaches the maximum of the excitation light conversion and the resulting CCT is minimal.

V. CONCLUSION

We discovered that the changes of spectral characteristics of the light emitted by a luminescent layer, which are related to the excitation wavelength, can be used to set the desired chromaticity temperature of the resulting white light. Our research revealed that for samples with a

weight ratio of 2:3 (U2:PDMS) and a luminescent layer thickness of about 126 μm we could use a variable excitation wavelength in the range of 425 - 445 nm approximately. In this case, we were able to set the CCT of white light in the field from 6905 K to 4387 K. Using samples with a weight ratio of 1:2 (U2:PDMS) and an average layer thickness of 119 μm we could use excitation wavelengths in the range of 425 - 465 nm, which correspond to the CCT settings ranging from approximately 34002 K to 4923 K (see Fig. 6 and Fig. 8, and Table 1). In this case, however, it is better to use excitation wavelengths in the range of 435 - 460 nm, which allow the tuning of the CCT of white light in the range of 8213 K to 4923 K (see Table 1).

Therefore, the appropriate luminescent layer parameters with a simultaneous choice of a suitable blue light source can produce a white light source with an adjustable CCT in the desired range of CCT values. This process can be used when designing white LED sources based on the blue-chip and luminescent layer with YAG:Ce phosphor and PDMS.

ACKNOWLEDGMENT

This article was supported by the Ministry of Education of the Czech Republic (Projects No. SP2018/170, SP2018/184, and SP2018/55). This work was supported by the European Regional Development Fund in the Research Centre of Advanced Mechatronic Systems project, project number CZ.02.1.01/0.0/0.0/16_019/0000867 within the Operational Programme Research, Development and Education.

REFERENCES

- [1] Q. Zhao, G. Jiang, Z. Wang, M. Shi, B. Yang, J. Zou, and T. Tu, "Chromaticity-tunable color converter of CaAlSiN₃:Eu²⁺ red phosphor film layer stacked YAG:Ce for warm-WLED," *Journal of Materials Science: Materials in Electronics*, vol. 29, no. 5, pp. 4011-4019, 2018.
- [2] H. Zhou, J. Zou, B. Yang, W. Wu, M. Shi, Z. Wang, Y. Liu, M. Li, and G. Zhao, "Facile preparation and luminescence performance of transparent YAG:Ce phosphor-in-tellurite-glass inorganic color converter for white-light-emitting diodes," *Journal of Non-Crystalline Solids*, vol. 481, pp. 537-542, 2018.
- [3] R. Zhang, B. Y. Wang, and H. Wang, "Advances in Phosphor-in-Glass for White LED," *Wuji Cailiao Xuebao/Journal of Inorganic Materials*, vol. 32, no. 4, pp. 337-345, 2017.
- [4] Z. Lin, H. Lin, J. Xu, F. Huang, H. Chen, B. Wang, and Y. Wang, "A chromaticity-tunable garnet-based phosphor-in-glass color converter applicable in w-LED," *Journal of the European Ceramic Society*, vol. 36, no. 7, pp. 1723-1729, 2016.
- [5] S. Li, Q. Zhu, D. Tang, X. Liu, G. Ouyang, L. Cao, N. Hirotsuki, T. Nishimura, Z. Huang, and R.-J. Xie, "Al₂O₃-YAG:Ce composite phosphor ceramic: A thermally robust and efficient color converter for solid state laser lighting," *Journal of Materials Chemistry C*, vol. 4, no. 37, pp. 8648-8654, 2016.
- [6] N. I. Fendinger, "Polydimethylsiloxane (PDMS): Environmental Fate and Effects. Organosilicon Chemistry Set," Weinheim, Germany: Wiley-VCH Verlag GmbH, ch.2, pp. 23-36, 2005.
- [7] S. W. Allison, F. Sabri, and P. Parajuli, "Exploration of thin polymer films for phosphor thermometry," *Advances in Technology to Support End User Mission*, in *Proc. of the 2016 Joint Conference/Symposium of the Society for Machinery Failure Prevention Technology and the International Society of Automation*, 2016.
- [8] F. Sabri, K. Lynch, R. Wilson, and S. W. Allison, "Sensing with phosphor-doped PDMS," in *Proc. 60th International Instrumentation Symposium*, IIS 2014, London, United Kingdom, 2014.
- [9] P. Parajuli, and S. W. Allison, "Spincoat-fabricated multilayer PDMS-phosphor composites for thermometry," *Measurement Science and Technology*, vol. 28, no. 6, 2017.
- [10] C. S. Burke, A. Markey, R. I. Nooney, P. Byrne, and C. McDonagh, "Development of an optical sensor probe for the detection of dissolved carbon dioxide," *Sensors and Actuators, B: Chemical*, vol. 119, no. 1, pp. 288-294, 2006.
- [11] Z. Xu, Z. Xia, and Q. Liu, "Two-step synthesis and surface modification of CaZnOS: Mn²⁺ phosphors and the fabrication of a luminescent poly (dimethylsiloxane) film," *Inorganic Chemistry*, vol. 57, no. 3, pp. 1670-1675, 2018.
- [12] L. C. Chen, W. W. Lin, and J. W. Chen, "Fabrication of GaN-based white light-emitting diodes on yttrium aluminum garnet-polydimethylsiloxane flexible substrates," *Advances in Materials Science and Engineering*, vol. 2015, Article number 537163, 2015.
- [13] J. Jargus, J. Nedoma, M. Fajkus, M. Novak, and V. Vasinek, "Study combination of luminophore and polydimethylsiloxane for alternative option of passive energy lighting," in *Proc. SPIE 10209*, 2017.
- [14] J. Jargus, J. Nedoma, M. Fajkus, M. Novak, L. Bednarek, and V. Vasinek, "Measurement of spectral characteristics and CCT mixture of PDMS and the luminophore depending on the geometric parameters and the concentration of the samples of the special optical fibers," in *Proc. SPIE 10232*, 2017.
- [15] A. Zukauskas, M. S. Shur, and R. Caska, "Introduction to solid state lighting," John Wiley & Sons, Inc., Canada, 2002.
- [16] S. Murai, K. Fujita, K. Iwata, and K. Tanaka "Optical properties of macroporous Y₃Al₅O₁₂ crystals doped with rare earth ions synthesized via sol-gel process from ionic precursors," *Optical Materials*, vol. 33, iss. 2, pp. 123-127, 2010.
- [17] Y. P. Fu, "Preparation of Y₃Al₅O₁₂: Ce powders by microwave-induced combustion process and their luminescent properties," *Journal of Alloys and Compounds*, vol. 414, iss. 1-2, pp. 181-185, 2006.
- [18] V. K. Kim, A. I. Zakharov, and V. A. Chaschin "Luminophores based on aluminum yttrium garnet (review)," *Glass and Ceramics*, vol. 71, no. 1-2, pp. 64-67, 2014.
- [19] D. Lin, P. Zhong, and G. He, "Color temperature tunable white LED cluster with color rendering index above 98," *IEEE Photonics Technology Letters*, vol. 29, iss. 12, 2017.
- [20] R. Srividya, C. P. Kurian, C. R. Srinivasan, and D. Velickovic, "Implementation of a tunable RGB LED light source," *International Journal of Control Theory and Applications*, vol. 8, no. 3, 2015.
- [21] M. V. Kisin, D. V. Mamedov, and H. S. El-Ghoroury, "Simulation of full-color III-nitride RGB LED," in *Proc. 16th International Conference on Numerical Simulation of Optoelectronic Devices*, NUSOD, Article number 7547069, pp. 137-138, 2016.
- [22] A. M. Colaco, C. P. Kurian, S. G. Kini, and S. G. Colaco, "CIE metrics to discover color rendering of RGB LEDs," *International Journal of Control Theory and Applications*, vol. 9, no. 39, 2016.
- [23] R. Malik, and S. Mazumdar, "Development of CCT tunable LED lighting system using red-blue-white LED," *Light and Engineering*, vol. 25, no. 4, 2017.
- [24] J. Oliva, A. Papadimitratos, E. de la Rosa Cruz, and A. Zakhidov, "Tuning color temperature of white OLEDs in parallel tandems," *Physica Status Solidi (A) Applications and Materials Science*, vol. 214, no. 11, 2017.
- [25] C. Li, R. S. Nobuyasu, Y. Wang, F. B. Dias, Z. Ren, M. R. Bryce, and S. Yan, "Solution-processable thermally activated delayed fluorescence white OLEDs based on dual-emission polymers with tunable emission colors and aggregation-enhanced emission properties," *Advanced Optical Materials*, vol. 5, no. 20, 2017.
- [26] Y. Bi, J. Ji, Y. Chen, Y. Liu, X. Zhang, Y. Li, M. Xu, Y. Liu, X. Han, Q. Gao, and H. Sun, "Dual-periodic-microstructure-induced color tunable white organic light-emitting devices," *Frontiers of Optoelectronics*, vol. 9, no. 2, 2016.
- [27] A. Zhou, F. Song, Y. Han, F. Song, D. Ju, K. Adnan, L. Liu, and M. Feng, "Color-tunable emission by adjusting sensitizer (Yb³⁺) and excitation power of 980 nm in NaGdTiO₄:Yb³⁺/Tm³⁺/Er³⁺

- phosphors for light emitting diodes," *Journal of Luminescence*, vol. 194, 2018.
- [28] J. Tang, J. Gou, G. Li, H. He, Y. Li, and C. Li, "Tunable upconversion luminescence from the phosphors of Yb³⁺, Tm³⁺ and Ho³⁺ tri-doped Re₂TeO₆ (Re = La, Gd, and Lu)," *Journal of Alloys and Compounds*, vol. 672, pp. 1-6, 2016.
- [29] H. Lin, D. Xu, D. Teng, S. Yang, and Y. Zhang, "Tunable multicolor and white-light upconversion luminescence in Yb³⁺/Tm³⁺/Ho³⁺ tri-doped NaYF₄ micro-crystals," *Luminescence*, vol. 30, no. 6, 2015.
- [30] J. Xu, L. Jia, N. Jin, Y. Ma, X. Liu, W. Wu, W. Liu, Y. Tang, and F. Zhou, "Fixed-component lanthanide-hybrid-fabricated full-color photoluminescent films as vapoluminescent sensors," *Chemistry - A European Journal*, vol. 19, no. 14, pp. 4556-4562, 2013.
- [31] F. Zhang, P. Yan, H. Li, X. Zou, G. Hou, and G. Li, "Towards full-color-tunable emission of two component Eu(III)-doped Gd(III) coordination frameworks by the variation of excitation light," *Dalton Transactions*, vol. 43, no. 33, pp. 12574-12581, 2014.
- [32] W. Niu, P. Yan, Z. Fan, N. Fan, J. Sun, and G. Li, "White-light luminescence of L-di-toluoyl-tartaric acid lanthanide complexes with 1d linear structure," *Science of Advanced Materials*, vol. 8, no. 12, pp. 2189-2196, 2016.
- [33] CIE Commission Internationale de l'Eclairage Proceedings, Cambridge University Press, Cambridge, 1931.
- [34] E. F. Schubert, *Light-Emitting Diodes*, Cambridge University Press, New York, 2nd edition, 2006.